Indoor Air 2009
www.blackwellpublishing.com/ina

INDOOR AIR
doi:10.1111/j.1600-0668.2009.00603.x

Viral kinetics and exhaled droplet size affect indoor transmission dynamics of influenza infection

Abstract The purpose of this paper was to investigate the effects of viral kinetics and exhaled droplet size on indoor transmission dynamics of influenza infection. The target cell-limited model with delayed virus production was adopted to strengthen the inner mechanisms of virus infection on human epithelial cell. The particle number and volume involved in the viral kinetics were linked with Wells-Riley mathematical equation to quantify the infection risk. We investigated population dynamics in a specific elementary school by using the seasonal susceptible – exposed – infected – recovery (SEIR) model. We found that exhaled pulmonary bioaerosol of sneeze (particle diameter < 10 μm) have 10^2-fold estimate higher than that of cough. Sneeze and cough caused risk probabilities range from 0.075 to 0.30 and 0.076, respectively; whereas basic reproduction numbers (R_0) estimates range from 4 to 17 for sneeze and nearly 4 for cough, indicating sneeze-posed higher infection risk. The viral kinetics and exhaled droplet size for sneeze affect indoor transmission dynamics of influenza infection since date post-infection 1–7. This study provides direct mechanistic support that indoor influenza virus transmission can be characterized by viral kinetics in human upper respiratory tracts that are modulated by exhaled droplet size.

S. C. Chen[1], C. P. Chio[2], L. J. Jou[3], C. M. Liao[2]

[1]Department of Public Health, College of Health Care and Management, Chung Shan Medical University, Taichung, Taiwan, [2]Department of Bioenvironmental Systems Engineering, National Taiwan University, Taipei, Taiwan, [3]Department of Biomechatronic Engineering, National Ilan University, Ilan, Taiwan

Key words: Indoor aerosol transmission; Viral kinetics; Influenza; Infectious droplets; Indoor air quality.

C. M. Liao
Department of Bioenvironmental Systems Engineering
National Taiwan University
Taipei
Taiwan 10617
Tel.: +886-2-2363-4512
Fax: +886-2-2362-6433
e-mail: cmliao@ntu.edu.tw

Received for review 9 June 2008. Accepted for publication 19 February 2009.

Practical Implications

This paper provides a predictive model that can integrate the influenza viral kinetics (target cell-limited model), indoor aerosol transmission potential (Wells-Riley mathematical equation), and population dynamic model [susceptible – exposed – infected – recovery (SEIR) model] in a proposed susceptible population. Viral kinetics expresses the competed results of human immunity ability with influenza virus generation. By linking the viral kinetics and different exposure parameters and environmental factors in a proposed school setting with five age groups, the influenza infection risk can be estimated. On the other hand, we implicated a new simple means of inhaling to mitigate exhaled bioaerosols through an inhaled non-toxic aerosol. The proposed predictive model may serve as a tool for further investigation of specific control measure such as the personal protection masks to alter the particle size and number concentration characteristics and minimize the exhaled bioaerosol droplet to decrease the infection risk in indoor environment settings.

Introduction

A number of studies have reported the factors involved in the aerosol transmission of infection in indoor environments. However, the viral kinetics of infectious diseases in human lung associated with the exhaled bioaerosol characteristics during the infectiousness periods is not well understood. To clearly quantify the risk of infection indoors for human infected influenza virus was valuable issues focusing on the correlation between the pulmonary mechanism, different human activities, and the critical exhaled virus droplet concentration.

Transmission of exhaled infectious diseases indoors has been receiving substantial attentions (Li et al., 2007; Nicas et al., 2005; Tang et al., 2006; Wan et al.,

2007; Xie et al., 2007). Infectious pathogens of these airborne transmittable diseases can originate from various sources in indoor environments, where human sources are found to be the major source (Cole and Cook, 1998). Influenza infection has been documented by aerosol exposure in the mouse model, the squirrel monkey model, and human volunteers (Douglas, 1975; Hayden et al., 1998; Knight, 1973; Snyder et al., 1986).

When influenza virus infected a healthy person, the multiple mechanisms were interacted among immunology, cells dynamics, and virus generation rate. Although there is no direct measurement of the infected cell mass, mathematical models have proven to be useful tools in the analysis of viral infections, immune response and pathogens (Perelson, 2002); explaining the biological phenomena and analyzing the experimental results. Recently, important results have been obtained in the mathematical modeling of viral dynamics for the HIV (Nowak and Bangham, 1996; Perelson et al., 1993, 1996, 1997), hepatitis B virus (HBV) (Marchuk et al., 1991; Nowak et al., 1996), hepatitis C (Neumann et al., 1998) and influenza infections (Baccam et al., 2006; Chang and Young, 2007; Hancioglu et al., 2007).

Baccam et al. (2006) had provided two models describing the kinetics of influenza A virus infection in human: a target cell-limited model and a target cell-limited model with delayed virus production. The results suggested that the model considering the delayed virus production was more realistic. Furthermore, the reasonable parameters of biological characteristics were derived from experimentally infected volunteers (Baccam et al., 2006; Murphy et al., 1980). Hence, the viral kinetics might affect the exhaled infectious droplet and even alter the infection risk.

Early researchers treated the upper respiratory tract (nose, mouth, and throat) was the primary location of droplet formation (Duguid, 1945, 1946; Loudon and Roberts, 1967). Humans and their activities are linked to a number of processes resulting in the introduction of droplets with infectious content into the indoor air. Hence, the influenza syndromes such as coughing and sneezing will of course generate the different characteristics of respiratory droplets. Nicas et al. (2005) presented the cumulative percentile by count versus initial (expelled) particle diameter based on the results of Duguid (1946).

Duguid (1946) indicated that the estimated lognormal distribution of respiratory droplet were geometric mean (GM) = 14 μm and geometric standard deviation (GSD) = 2.6 for cough and GM = 8.1 μm and GSD = 2.3 for sneeze. On the other hand, Loudon and Roberts (1967) shown that the estimated lognormal parameters was GM = 12 μm and GSD = 8.4 for cough. More recently, Papineni and Rosenthal (1997) measured expired bioaerosol droplets (in nose and mouth breathing, coughing and talking) to be <2 μm in size, with no droplets >8 μm. Hence, the viral kinetics and particle size diameters may play the critical roles for evaluating the infection risk.

Our previous researches have focused on the transmission models and control measures modeling by integrating the Wells-Riley mathematical model and susceptible-exposed-infected-recovery (SEIR) model to estimate the winter/summer and age group-specific risk of infections in indoor environments (Chen and Liao, 2008; Chen et al., 2006; Liao et al., 2008). We conducted the indoor environments factors of a real elementary school and etiological characteristics of influenza to estimate the age-specific risk of infection (P) and basic reproduction number (R_0). The estimate of R_0 is defined as the average number of successful secondary infections cases generated by a typical primary infected case in an entirely susceptible population (Anderson and May, 1991). An average R_0 of 1 means the disease is endemic equilibrium within the population. R_0 essentially determines the rate of spread of an epidemic and how intensive a policy will need to be to control the epidemic (Ferguson et al., 2003).

Taken together, we try to strengthen the inner mechanisms of virus infection on human epithelial cell and clearly quantify the human activities that may affect the exhaled virus droplet concentration and linking the concept with our previous study. The objective of this study was to explore a framework to clearly quantify the infection risk based on the relationships among exhaled pulmonary bioaerosol and viral kinetics of airborne influenza virus during infection within an individual.

Materials and methods

The aerosol transmission dynamics approach can be divided into three phases (Figure 1). We conducted the target cell-limited model with delayed virus production associated with the related fitted parameters to estimate the influenza viral kinetics (Figure 1a). We combined the particle size distribution and different human activities to estimate the exhaled pulmonary bioaerosol dynamics (Figure 1b). We finally estimated the risk of infection based on aerosol transmission dynamics (Figure 1c).

Influenza viral kinetics

We linked a model of acute viral infection that incorporates target cell-limited model with the results of experimental human infection (Baccam et al., 2006) to quantitatively describe the influenza viral kinetics. The target cell-limited model with delayed virus production can quantify the number of uninfected cell, infected cell, producing-virus infected cells, and infectious virus titers when influenza A virus infected the human epithelia lung cells (Figure 1a),

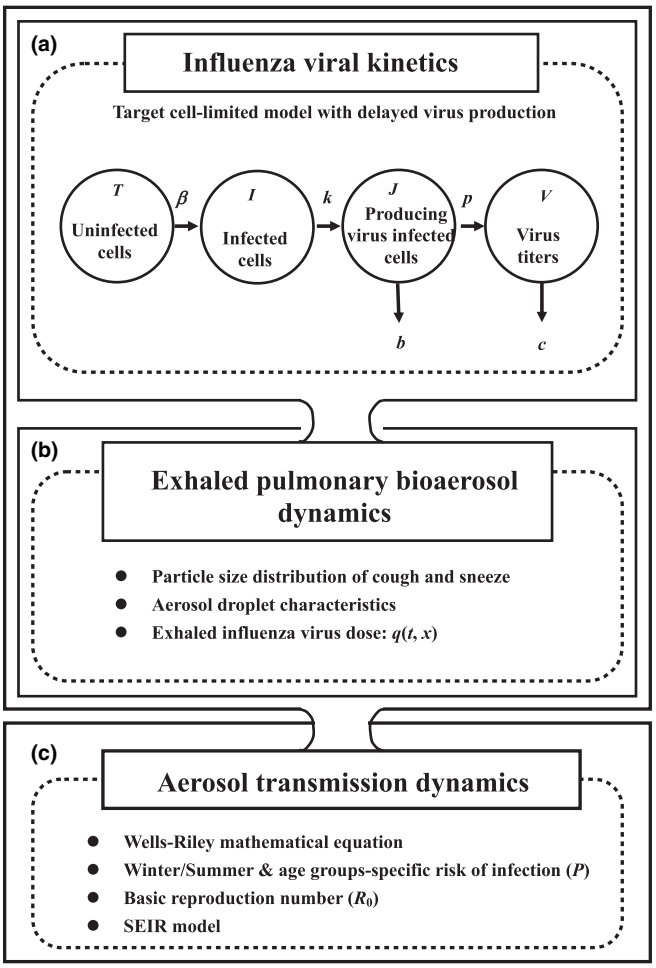

Fig. 1 Schematic showing the indoor airborne infectious droplets transmission including the (a) Influenza viral kinetics, (b) Exhaled pulmonary bioaerosol dynamics, and (c) Aerosol transmission dynamics

$$\frac{dT_C}{dt} = -\beta T_C V_C, \tag{1}$$

$$\frac{dI_C}{dt} = \beta T_C V_C - kI_C, \tag{2}$$

$$\frac{dJ_C}{dt} = kI_C - bJ_C, \tag{3}$$

$$\frac{dV_C}{dt} = pJ_C - cV_C, \tag{4}$$

where T_C is the number of uninfected target cells (#), I_C is the number of infected cells but not yet producing virus (#), J_C is the number of infected cells actively producing virus (#), and V_C is the infectious viral titer of nasal wash expressed as 50% tissue culture infective doses (TCID50/ml).

Table 1 Best-fitted parameter values for the target cell-limited model with a delay[a]

Name	Description (unit)	Geometric mean (95% CI)
T_0	The number of uninfected target cells (#)	4×10^8
V_0	The infectious viral titer of nasal wash (TCID50/ml)	7.5×10^{-2} (7.6×10^{-4}–7.5)
β	The rate constant characterizing infection ((TCID50/ml)/day)	3.2×10^{-5} (6.0×10^{-6}–1.7×10^{-4})
k	The average transition rate from I to J (per day)	4.0 (3.0–5.2)
p	The average rate of per cell shedding infectious virus titers (TCID50/ml/day)	4.6×10^{-2} (1.2×10^{-2}–1.7×10^{-1})
b	The death rate of infected cells (per day)	5.2 (3.2–8.6)
c	The clearance rate of virus (per day)	5.2 (3.1–8.7)

[a]Adopted from Baccam et al. (2006).

The experimental infection study of H1N1 influenza virus were $10^{4.2}$ (TCID50/ml) of cloned wild-type influenza A/Hong Kong/123/77 (Baccam et al., 2006). The other estimated parameters of the target cell-limited model with delayed virus production are defined in Table 1. The system of first-order ODEs was solved by using Berkeley Madonna (Version 8.0.1).

Quantum generation rate varied with particle size and date post-infection

Predicting infection risk for a susceptible person involves a set of factors including the airborne concentration of pathogens carried on particles with diameter ≤ 10 μm. Previous studies (Atkinson and Wein, 2008; Duguid, 1945, 1946; Loudon and Roberts, 1967) indicated that particle diameter emitted by cough and sneeze was nearly 10 μm. Here, we defined the quantum generation rate is the function of the expulsion event rate F (event/h) by cough or sneeze associated with the time-dependent virus concentration in respiratory fluid C_t (TCID50/ml). Total particle volume per expulsion event is the product of the mean particle volume ($\bar{v}_x$) and the number of particles in each particle diameter (N_x). The sum of the total particle volume expressed as $N_x \times \bar{v}_x$ (10^{-10} ml). The quantum generation rate (TCID/h) varying with the day post-infection (t) and particle diameter x ($x \leq 10$ μm), therefore, has the form as,

$$q(t,x) = F \times C_t \times N_x \times \bar{v}_x. \tag{5}$$

We recognized that the present used target cell-limited model with delayed virus production model well describes the target cell viral kinetics in human upper respiratory tract (Baccam et al., 2006). On the other hand, C_t represents the virus concentration in respiratory fluid and is directly correlated to exhaled bioaerosol droplets ($q(t,x)$). Thus a time-profile of

virus concentration in respiratory fluid C_t in Equation (5) can be obtained by best fitting a model to viral kinetic data based on Baccam et al. (2006). To quantitative expiratory droplet characteristics, we adopted the valuable experimental data from Duguid (1946) and Loudon and Roberts (1967) to describe the relationship between particle size diameter and droplet number concentration of cough and sneeze, respectively. The relationship between particle initial volume and number of particles emitted per cough was adopted from Loudon and Roberts (1967). Software Table Curve 2D was used to perform the fitting techniques.

ing any natural die-off of the airborne infectious agents and natural depositional losses. Furthermore, Riley et al. (1978) made two salient assumptions to quantify the indoor respiratory infections. The first assumption implies that an infectious droplet nucleus has an equal chance of being anywhere within a building's airspace, whereas the second assumption implies that the quantum concentration and the outdoor air supply rate remain constant with time.

We modified the Wells-Riley mathematical equation proposed by Rudnick and Milton (2003) to estimate the transmission potential of influenza virus in elementary classroom,

$$P(t,x) = \frac{D}{S} = 1 - \exp\left\{-\frac{Iq(t,x)p_iT}{Q}\left\{1 - \frac{V}{QT}\left[1 - \exp\left(-\frac{QT}{V}\right)\right]\right\}\right\}, \quad (6)$$

Quautitative exhaled bioaerosol infections

Our study was conducted at the Ming-Chuan elementary school located in southern Taipei city. Of 494 students including 60 kindergarten and 434 elementary students are appointed in four buildings. The average numbers of students in each classroom are 30, 23, 26, and 30 for 1st–2nd, 3rd–4th, 5th–6th grades, and kindergarten class, respectively, in that schoolchildren are classified into four age categories, with kindergarten of 4–6 years and elementary students of 7–8, 9–10, and 11–12 years, whereas the staff and administrative staff of 25–45 years is also included. Here we consider the kindergarten is an enclosed space with a ventilation system that differs from the natural-forced combined ventilation performance for general elementary classroom. In the exposure duration, each class has 40 min with a 5–10 min recess time. Total exposure times in classroom are nearly 0.28, 0.25, and 0.11 days for kindergarten students, elementary students, and staff and administrative staff, respectively.

The emitted pathogen concentration affected by many factors such as the ventilation situation, human activities behaviors, natural depositional losses, and removal phenomena. To simplify the model, we used the Wells-Riley equation to describe the risk of infection in indoor environments. The mass balance in the original Wells-Riley equation accounts only for infectious agent removal from the indoor air by ventilation. We neglected removal phenomena including any natural die-off of the airborne infectious agents and natural depositional losses. Furthermore, Riley et al. (1978) made two salient assumptions to quantify the indoor respiratory infections. The first assumption implies that an infectious droplet nucleus has an equal chance of being anywhere within a building's airspace, whereas the second assumption implies that the quantum concentration and the outdoor air supply rate remain constant with time.

We modified the Wells-Riley mathematical equation proposed by Rudnick and Milton (2003) to estimate the transmission potential of influenza virus in elementary classroom,

$$P(t,x) = \frac{D}{S} = 1 - \exp\left\{-\frac{Iq(t,x)p_iT}{Q}\left\{1 - \frac{V}{QT}\left[1 - \exp\left(-\frac{QT}{V}\right)\right]\right\}\right\}, \quad (6)$$

where P is the probability of infection for susceptible population varied with particle size and date post-infection, D is the number of cases among S persons susceptible to the infection, S is the number of susceptible, I is the number of sources of infection, $q(t,x)$ is the particle diameter/date post-infection-dependent quantum generation rate by an infected person (TCID50/h), p_i is the breathing rate per person (m^3/d), T is the time of exposure per unit of time (d), Q is the fresh air supply rate (m^3/day) that removes the infectious aerosol in volume per unit of time, and V is the volume of the ventilated space (m^3).

For modeling the respiratory infection, we incorporate initial $I = 1$ and $S = n - 1$ into Equation (6) to estimate R_0 for five age groups 4–6, 7–8, 9–10, 11–12 and 25–45 years at an elementary school,

$$R_0(t,x) = (n-1)\left\{1 - \exp\left\{-\frac{q(t,x)p_i\mathrm{T}}{Q}\left[1 - \frac{V}{QT}\left(1 - \exp\left(-\frac{QT}{V}\right)\right)\right]\right\}\right\}, \quad (7)$$

where the symbol of n represents the total number in our modeling ventilation airspaces. The winter/summer and age-specific R_0 value among schoolchildren can be estimated by taking into account indoor environmental ventilation, number of students, and quantum generation rate by infectious person, to describe the risk in specific space.

Indoor aerosol transmission

We used the susceptible-exposed-infected-recovery (SEIR) model to simulate the dynamic of infected population. Compartments S, E, I, and R are used for

the epidemiological classes. The SEIR model can provide a basic description of the transmission dynamics of pandemic influenza by using a simple parameterized set of ordinary differential equations,

$$\frac{dS}{dt} = \mu N - \beta_i IS - \mu S, \tag{8}$$

$$\frac{dE}{dt} = \beta_i IS - \sigma E - \mu E, \tag{9}$$

$$\frac{dI}{dt} = \sigma E - \upsilon I - \mu I, \tag{10}$$

$$\frac{dR}{dt} = \upsilon I - \mu R, \tag{11}$$

$$N(t) = S(t) + E(t) + I(t) + R(t), \tag{12}$$

where $N(t)$, $S(t)$, $E(t)$, $I(t)$, and $R(t)$ are the number of total population, susceptible, exposed, infected, and recovery at time t for age groups-specific, respectively, β_i is transmission coefficient representing the probability that an infected will have contact with and successfully infect a susceptible, σ is the rate at which an exposure individual becomes infectious per unit time that is equal to 0.333/d (Anderson and May, 1991), υ is the rate at which an infectious individual recovers per unit time (per day) that is equal to 0.143 (1/average infectiousness periods of 7 days), and μ is the birth rate and death rate that is equal to 0.013/year (http://www.mio.gov.tw/stat/). The spread of an infectious disease in a population of host individuals reflects whether or not the virus can grow and establish an infection. The crucial quantity can be characterized by basic reproduction number R_0 and mathematically expressed as $R_0 = (\beta_i \times N)/\mu + \upsilon$ (Anderson and May, 1991).

Results

Exhaled bioaerosol droplets

Figure 2a,c give the original experimental data from Loudon and Roberts (1967) and Duguid (1946) describing the size-dependent particle number for cough and sneeze, respectively. Observably, the particle numbers are approximately 10^5 for sneeze and 10^2 for cough, a sneeze releases approximately three-fold order more particles than that of a cough. The best-fitted models were derived for cough and sneeze associated with the peak function with high $r^2 = 0.97$ and 0.99, respectively (Table 2, Equations (T1) and (T2), Figure 2b,d).

Estimates for the exhaled bioaerosol droplets are available in that our assessment allows us to determine the time-dependent virus concentration in respiratory fluid C_t (TCID50/ml) (Figure 3a). The calculation is based on the target cell-limited model with delayed virus production [Equations (1)–(4)] with the geometric mean parameters estimates given in Table 1. Fitted equation of time-dependent virus concentration in respiratory fluid is expressed as Equation (T3) with lognormal distribution. With considering the influenza viral kinetics in target cells, the patterns started after day 1 and approached to highest virus concentration during day 2–3 post of infection with 7.5×10^5 TCID50/ml, and slowly decreased to <1 TCID50/ml (Figure 3a). It indicated that the virus replication in human epithelia lung cells is much more rapid than initially virus load ($V_0 = 7.5 \times 10^{-2}$). The kinetics of target cells in human lung can clearly demonstrate the virus kinetics when the influenza virus attacks our lung tissue cells. The number of time-dependent uninfected target cells, infected cells but not yet producing virus, and infected cells actively producing viral are presented in Figure 3b.

Here the size-dependent particle volume is also presented. We best fitted a nonlinear model to the data (Loudon and Roberts (1967)) describing the relationship between the particle diameters corresponding to the particle initial volume per cough (Table 2, Equation (T4), Figure 3c). We assumed that the fitted model of size-dependent particle volume can applied to sneeze. Hence, the size-dependent total particle volume for cough and sneeze are presented in Figure 3d,e [Equations (T5 and T6)] by integrating the size-dependent particle volume and the size-dependent particle numbers (Figures 2b,d and 3c), respectively. The highest total volume occurs at $x = 5.8$ μm (volume $= 500 \times 10^{-10}$ ml) and $x = 26$ μm (volume $= 3 \times 10^{-7}$ ml) for cough and sneeze, respectively. These results may imply that the infectious viral titer of nasal wash can emit higher level at sneeze than those of cough. However, as we will explain, the large particle in respiratory aerosol might deposit quickly while the particle diameter is increased.

Modeling quantum generation rate

Figure 4 demonstrates the interesting dynamic behavior of the model fitting quantum generation rate ($q(t,x)$) of influenza virus presented as contour and surface response. Figure 4 shows that the date post-infection and particle size-dependent function associated with an exhaled frequency can be present reasonably well by Equation (5). The results is integrated the frequency of cough or sneeze per hour (F), time-dependent virus concentration in respiratory fluid [Equation (T3)], and size-dependent total particle volume [Equations (T5) and (T6)]. In this study, the parameter F is assumed to be 50 and 1/h for cough and sneeze, respectively. We noted that the highest quantum generation rate is estimated to be 0.57 TCID50/h

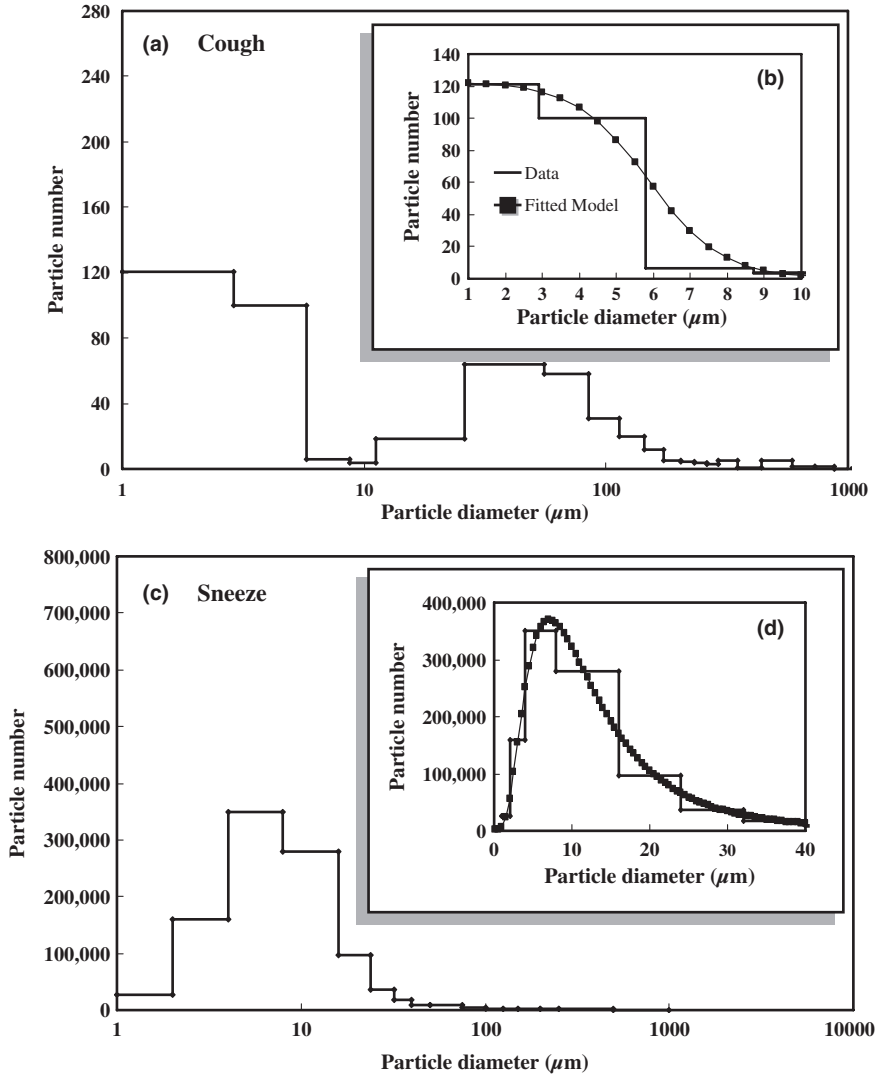

Fig. 2 Size-dependent particle number for cough and sneeze. In (a) and (c) are shown the original experimental data for cough and sneeze from Loudon and Roberts (1967) and Duguid (1946), respectively. In (b) and (d) are shown the fitted models from diameter 0 to 10 μm and 0 to 40 μm for cough and sneeze, respectively

Table 2 Optimal fitted equations of particle number, time-dependent virus concentration in respiratory fluid, size-dependent total particle volume per expulsion event of cough and sneeze

Type	Fitted equation[a]	r^2	
Particle number			
Cough	$N_x = (0.00812 + 0.0000233\exp^x)^{-1}$	0.97	(T1)[b]
Sneeze	$N_x = 2123 + 367734\exp\left(-0.5(\ln(x/7.11)/0.65)^2\right)$	0.99	(T2)[c]
Time-dependent virus concentration in respiratory fluid			
	$\log(C_t) = LN(-12.27, 17.63, 2.64, 8.41, 1.98)$	0.99	(T3)[d]
Size-dependent particle volume			
	$\bar{v}_x = 1.3852 + 0.0341x^3$	0.97	(T4) [c]
Size-dependent total particle volume			
Cough	$N_x\bar{v}_x = LN(109.59, 393.11, 5.71, 4.30, 0.75)$	0.99	(T5)[d]
Sneeze	$N_x\bar{v}_x = LN(232283.11, 31368754.02, 27.29, 53.33, 2.44852)$	0.99	(T6)[d]

[a] N_x is the particle numbers at specific particle diameter x (μm), C_t is the virus concentration in respiratory fluid (TCID50/ml) at specific time t (d), $\bar{v}_x$ is the particle volume at specific particle diameter x (μm), and $N_x\bar{v}_x$ is total particle volume at specific particle diameter x (μm).
[b] Based on data from Loudon and Roberts (1967).
[c] Based on data from Duguid (1946).
[d] $\mathrm{LN}(a, b, c, d, e) = a + b\exp(-\ln 2\ln\left(1 + (x - c)\left(e^2 - 1\right)/(de)\right)^2\ln(e)^2)$.

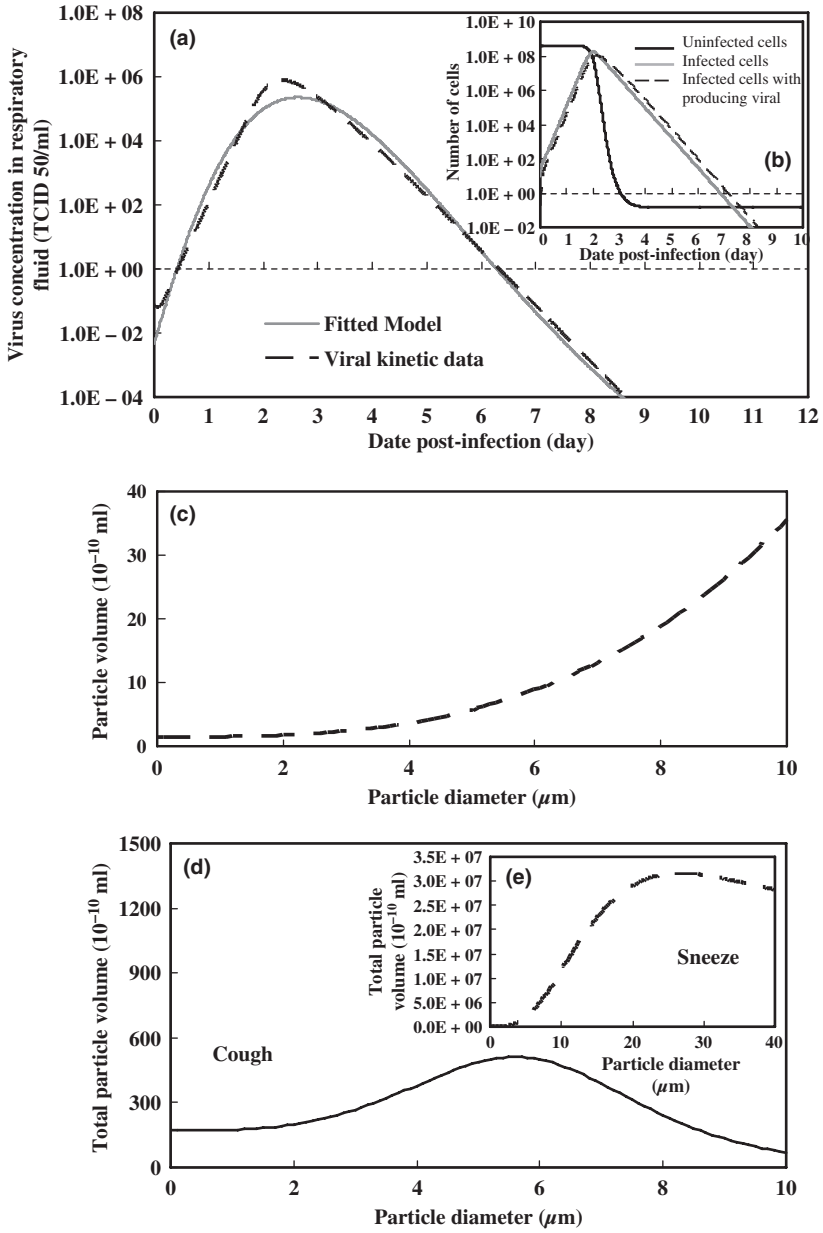

Fig. 3 (a) We fitted the function to the time-dependent virus concentration in respiratory fluid (TCID50/ml). (b) The number of time-dependent uninfected target cells, infected cells but not yet producing virus, and infected cells actively producing viral are presented by the virus kinetics equations [Equations (1)–(4)]. (c) We best fitted a model to the data [Loudon and Roberts (1967)] describing the relationship between the particle diameters corresponding to the particle initial volume per cough. (d) and (e) shown the size-dependent total particle volume for cough and sneeze, respectively

at $x = 5.5$ μm at day 2.6 post-infection for cough behavior, whereas sneeze is nearly 264 TCID50/h at $x = 10$ μm at day 2.6 post-infection (Figure 4). In the periods of infectiveness at day 1–4 post-infection, the ranges of quantum generation rate are estimated from 0.057 to 0.224 TCID50/ml at $x = 5.5$ μm for cough behavior, whereas those of sneeze are estimated from 26.69 to 104.19 TCID50/ml at $x = 10$ μm. Observably, larger quantum generation rate of sneeze than that of cough may be caused by a great quantity of emitted particle numbers and total particle volume.

Indoor aerosol transmission potential

Table 3 shows the input parameters used in Wells-Riley mathematical equation for five age groups. The environmental factors were estimated based on the Ming-Chung elementary school scenario with actual classroom size and attended schoolchildren in the ventilated airspace. The breathing rates are adopted from ICRP 66 (International Commission on Radiological Protection, 1994) for different age groups. The ventilation rates are reasonably assumed to be 2 and 3

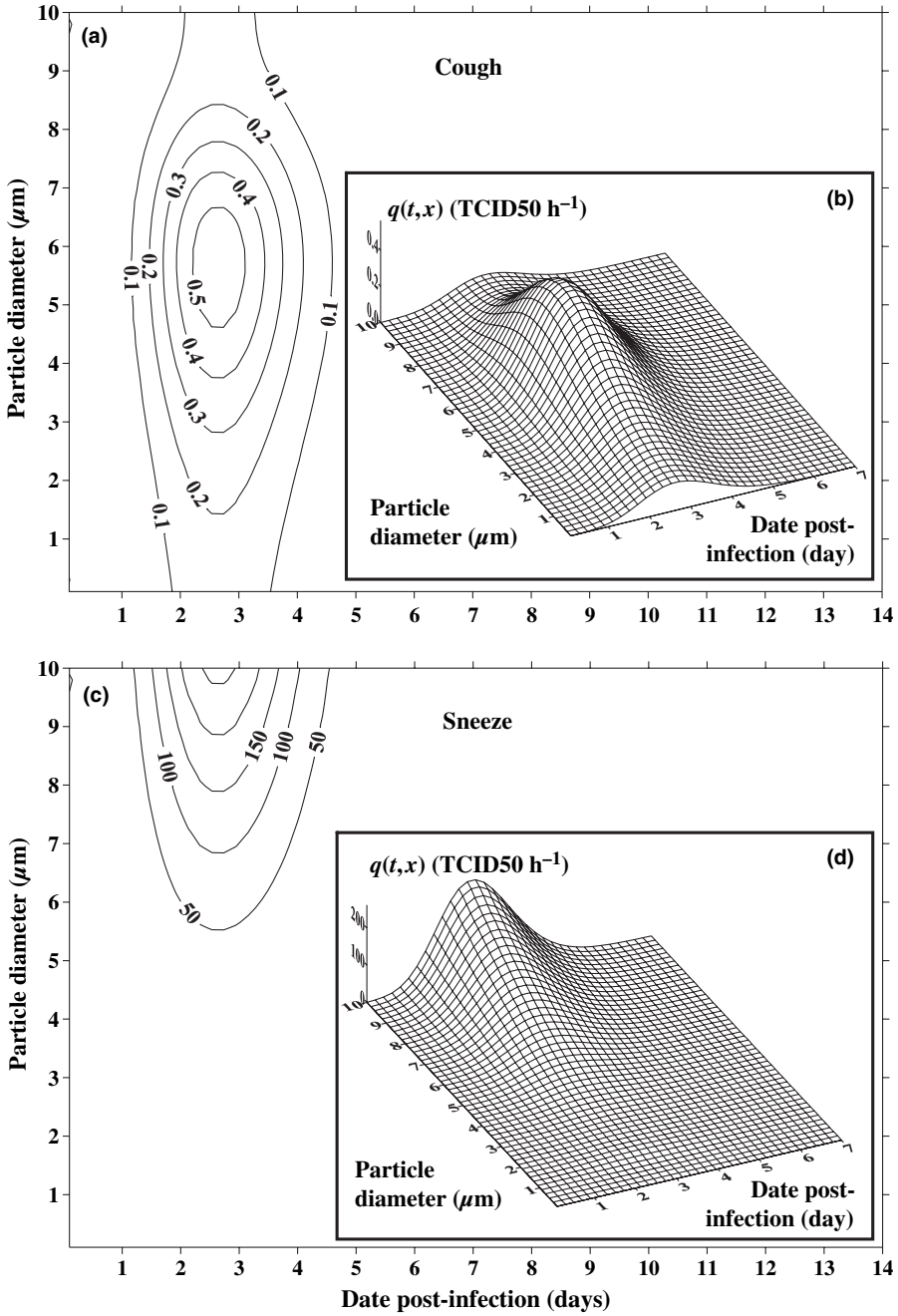

Fig. 4 Contours (a, c) and surface response (b, d) of quantum generation rate $q(t,x)$ for cough and sneeze

Table 3 Input parameters used in Wells-Riley mathematical equation for five age groups in an elementary school

	Unit and symbols years	Kindergarten 4–6 years	First–second 7–8 years	Third–fourth 9–10 years	Fifth–sixth 11–12 years	Teaching and administrative staff 25–45 years
Season (Winter = W, Summer = S)		W, S	W, S	W, S	W, S	W, S
People in the ventilated airspace	n	60	30	23	26	40
Number of infectors	i	1	1	1	1	1
Volume of the shared airspace	V (m^3)	1013	245	245	245	732
Total exposure time	T (d)	0.28	0.25	0.25	0.25	0.11
Breathing rate	p_i (m^3/day)	N (7.68, 0.15)[a]	N (8.4, 0.08)	N (9.12, 0.16)	N (10.56, 0.08)	N (11.16, 0.20)
Ventilation rate	Q (m^3/day)	48628, 97257	17614, 35228	17614, 35228	17614, 35228	52704, 105408

[a]N($\bar{x}$, SD) = Normal distribution with mean and standard deviation.

Table 4 Seasonal risk of infection and basic reproduction number in five age groups

	Kindergarten	First–second	Third–fourth	Fifth–sixth	Teaching and administrative staff
Risk of infection (P)					
Cough (diameter <10 μm)					
Summer					
Min	0.0375	0.0278	0.0278	0.0278	0.0645
Max	0.0378	0.0285	0.0286	0.0288	0.0647
Winter					
Min	0.0749	0.0556	0.0556	0.0556	0.129
Max	0.0755	0.0571	0.0572	0.0575	0.1292
Sneeze (diameter <10 μm)					
Summer					
Min	0.0375	0.0278	0.0278	0.0278	0.0645
Max	0.1627	0.334	0.3553	0.3958	0.1298
Winter					
Min	0.0749	0.0556	0.0556	0.0556	0.129
Max	0.2999	0.5569	0.5847	0.6352	0.2463
Basic reproduction number (R_0)					
Cough (diameter <10 μm)					
Summer					
Min	2.21	0.81	0.61	0.70	2.52
Max	2.23	0.83	0.63	0.72	2.52
Winter					
Min	4.42	1.61	1.22	1.39	5.03
Max	4.46	1.66	1.26	1.44	5.04
Sneeze (diameter <10 μm)					
Summer					
Min	2.21	0.81	0.61	0.70	2.52
Max	9.60	9.69	7.82	9.90	5.06
Winter					
Min	4.42	1.61	1.22	1.39	5.03
Max	17.70	16.15	12.86	15.88	9.61

ACH/h for summer and winter, respectively. We incorporated the parameters values (Table 3) into Equations (6) and (7) to estimate the risk of infection (P) and the age-group specific basic reproduction number (R_0), respectively. The major results shown in Table 4 can be summarized as follows: (a) The range (min–max) of the P and R_0 estimates of cough and sneeze indicate that the P (highest value = 0.6352) and R_0 (highest value = 17.70) estimates are higher in winter than those in summer for all five age groups; (b) Higher potential for transmission influenza virus focused on the youngest kindergarten age groups (R_0 ranges from 4.42 to 17.70 for sneeze); and (c) The P ranges between 0.0749 and 0.2999 for sneeze and 0.0749 and 0.0755 for cough, whereas R_0 ranges between 4.42 and 17.70 for sneeze and 4.42 to 4.46 for cough.

In order to assess whether the size-dependent and post-infection will affect the estimations of P and R_0, we illustrated the P and R_0 values corresponding to seasonal variation with different activities for specific kindergarten age groups (Figure 5). The specific particle diameter ranged from 0.5 to 10 μm, indicating slightly impact on the P and R_0 values by the variation of particle diameter (Figure 5a,b,e,f). On the other hand, for sneeze, higher P and R_0 values occurred at day 2–3 post-infection compared with that of the other days of infection (Figure 5c,d,g,h). The seasonal transmission dynamics in kindergarten are illustrated in Figure 6 based on the applied SEIR model [Equations (8)–(12)] and input parameters (Table 3). The expected infected numbers are estimated to be 28 and 23 in winter/summer for cough and 31 and 30 in winter/summer for sneeze in overall 60 number populations.

Discussion

Mathematical modeling for virus kinetics

Over the years, only three types of mathematical approaches have been developed to describe the influenza virus kinetics within a single infected host. The first of these papers (Bocharov and Romanyukha, 1994) provides a comprehensive system of differential equations representing 13 variables and 60 parameters. The second paper used several cellular automaton simulations to include spatial effects and to visualize the spread of the infection in lung epithelial tissue (Beauchemin et al., 2005). Baccam et al. (2006) used five state variables and 10 parameters which are the potentially most important for understanding the time course of influenza A infection. Generally, the

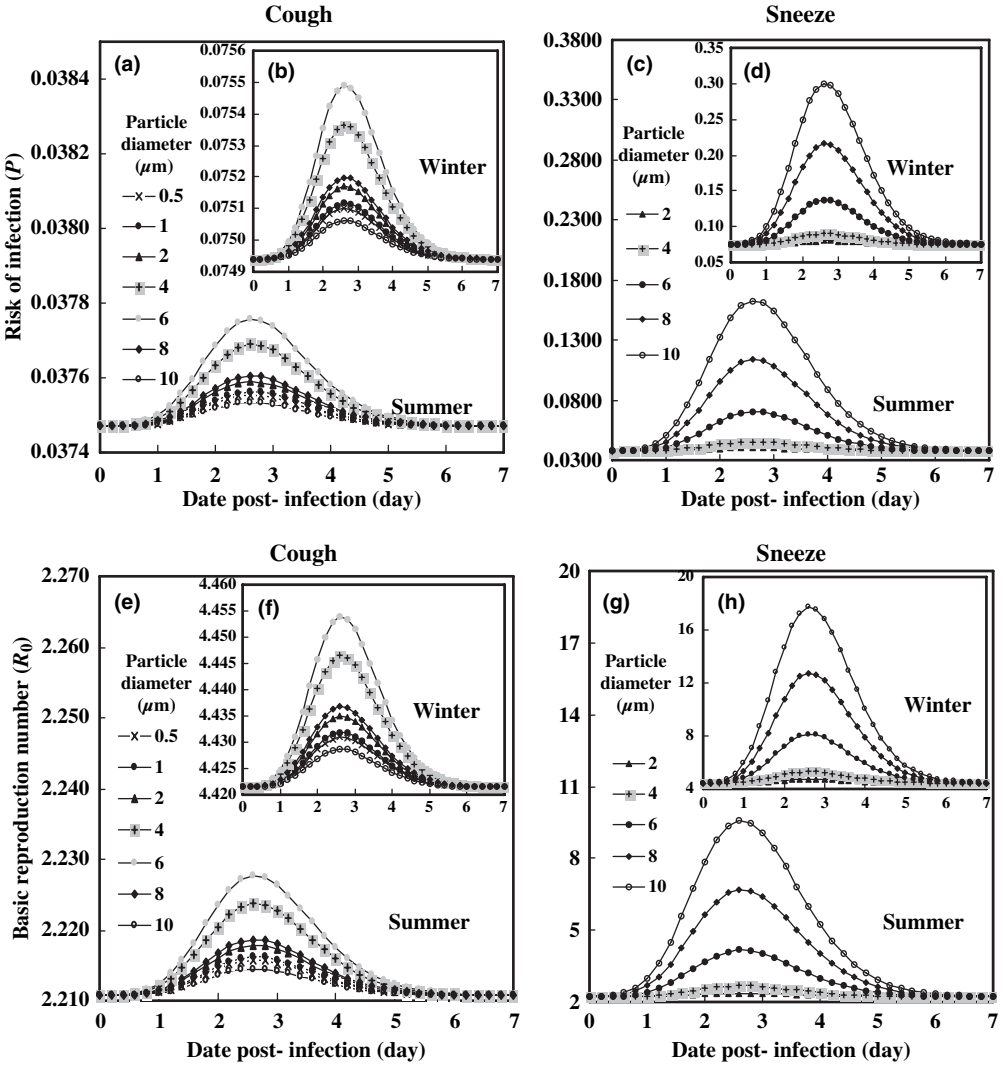

Fig. 5 Seasonal and size dependent risk of infections (a–d) and basic reproduction numbers (e–h) for cough and sneeze. The particle sizes ranged from 0.5, 1, 2, 4, 6, 8, and 10 μm

complexity of mathematical methods, the accurate estimations of available parameter, and the human biological mechanism on containing influenza A virus are equally important.

There were limitations presented in the target cell-limited model with delayed virus production. The data we evaluated were derived from experimentally infected subjects given intranasal challenge, which generally results in upper respiratory tract infection. In contrast, natural influenza infection most likely involves lower respiratory tract, i.e., trachea bronchial and viral replication (Baccam et al., 2006). Hence, Influenza A virus is limited by the availability of susceptible target (epithelial) experimental data. The second limitation is that we neglected the free virus migrates into a new area, then the number of susceptible target cells increases allowing the virus to undergo another surge in viral titer (Baccam et al., 2006).

Strictly speaking, the biological parameters of the target cell-limited model with delayed virus production can strengthen three issues on initial viral loads V_0 and clearance rate c. Chang and Young (2007) modeled the different initial dose to estimate the time course of infected cells and to develop the simple scaling law for the severity and characteristic time scales of influenza A infection in man. Focusing on the clearance rate c, Chang and Young (2007) also promoted that the interferon (IFN) immunity and cytotoxic T-lymphocytes (CTLs) immunity both play an important role in combating influenza A. Hancioglu et al. (2007) advance dynamically modeled the complicated immune response to humans in that the three important components of the immune response: the interferon immunity by moving the healthy cell that virus needs for reproduction, cellular immunity by removing the infected cells, and the adaptive immunity by lowering the effective concentration of the virus. Handel et al. (2007) also combine data from influenza infections of human volunteers with a mathematical framework that allows estimation of the parameters that govern the

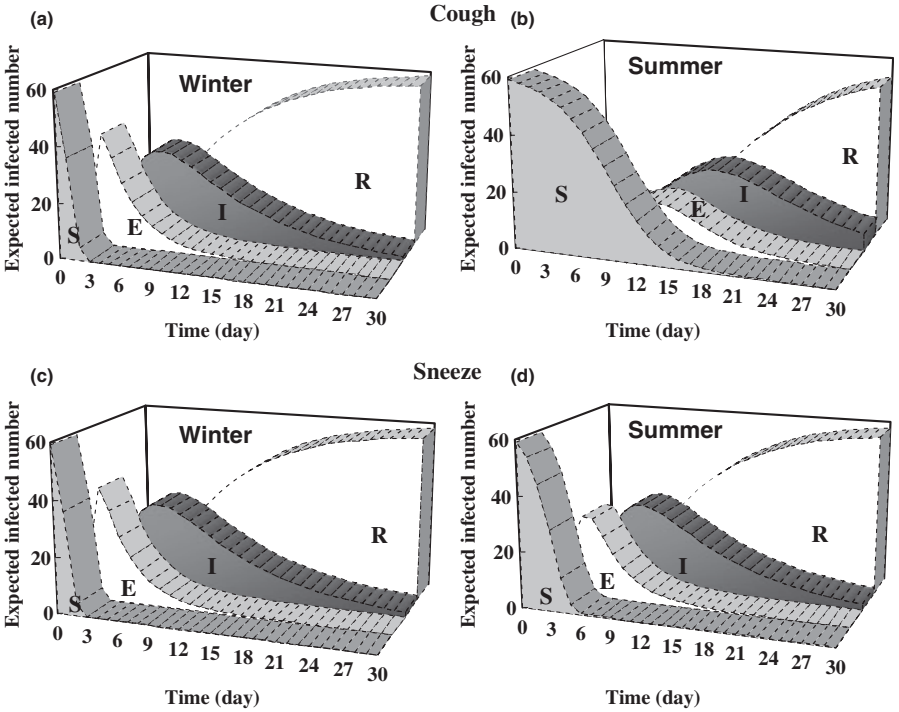

Fig. 6 Expected infected number for cough and sneeze by SEIR model in winter (a, c) and summer (b, d)

initial generation and subsequent spread of neuraminidase inhibitor resistance in influenza. In the present work, the infection would die from the lack of new cells to infect, rather than as a result of immune attacks. This could be the subject of future research.

Quantify exhaled bioaerosol droplets

To accurately estimate the exhaled bioaerosol droplets ($q(t,x)$) are based on the assumptions of the function of the expulsion event rate F (event/h), time-dependent virus concentration in respiratory fluid C_t (TCID50/ml), and the total particle volume per expulsion event. Exhaled bioaerosols droplets are formed in the respiratory tract, upon inspiration and expiration, as a consequence of momentum transfer from air flowing through the lungs to the airway lining fluid. However, it is difficult to validate the assumed results with lacking experimental data of the exhaled virus-carrying droplets in indoor environments. Actually, we could not fully understand what chemical or physical variation on virus through the lung cell to exhaled organ such as mouth or nose.

In our study, we focused only on direct transmission of infection droplet diameter <10 μm including the 'aerosol transmission' (Transmission occurs via large droplets (≥ 5 μm diameter) generated from the respiratory tract of the infected individual during coughing or sneezing, talking, or during procedures) and 'droplet transmission' (Transmission occurs via the dissemination of microorganisms by aerosolization). Hinds (1999) had characterized the property of bioaerosols, and also indicated that most airborne 20–300 nm-sized viruses were the part of droplet nuclei or attached to other particles, namely the carrying-virus particles or droplets. These viruses were transmitted to other host by inhaling these airborne droplets, and the aerosolization process of airborne droplets might include cough, sneeze, or talk. Edwards et al. (2004) hypothesize that, by altering lung airway surface properties through an inhaled non-toxic aerosol, we might substantially diminish the number of exhaled bioaerosol droplets and thereby provide a simple means to potentially mitigate the spread of airborne infectious disease independently of the identity of the airborne pathogen or the nature of any specific therapy. In our conceptual model assumptions, hence, the influenza viral kinetics only considered the transmission to other (or spray out) through cough and sneeze.

Transmission potential of cough and sneeze

Why the basic reproduction number of sneezes is higher than that of cough? The results may be caused by the higher particle number concentration of sneeze and the higher total particle volume. Particle diameter and environmental factors also play the roles on transmission potential. Several researches extended the classical study of the *Wells evaporation-falling curve* (Fennelly et al., 2004; O'Grady and Riley, 1963; Wells, 1934; Xie et al., 2007) of droplet considering the airborne transmission and transmission by large droplets. Atkinson and Wein (2008) implicated that a close unprotected horizontally-directed face-to-face sneeze is

potent enough to cause droplet transmission with an airborne particle size <20 μm, whereas from a close unprotected cough appears to be not significant. A droplet nucleus is the airborne residue of a potentially infectious (microorganism bearing) aerosol from which most of the liquid has evaporated (Nicas et al., 2005; Wells, 1934). This curve shows the time to evaporate completely varied with the droplet diameter, i.e., the deposition and evaporation mechanism of the droplet in indoor might be an function of many physical parameters, such as relative humidity, the ambient air velocity, ambient air temperature, etc (Xie et al., 2007). Expired bioaerosols can also travel great distances and remain airborne for an extended period of time, particularly when droplet diameters are too large for diffusive deposition (>200 μm) or too small for gravitational deposition (<2 um) (Gerrity et al., 1979; Stahlhofen et al., 1989). Fiegel et al. (2004) also mentioned several unresolved issue including the distribution of airborne viruses within expired bioaerosol droplets; the life-times of airborne pathogens as a function of droplet diameter, distance traveled and environmental conditions; and the general threat of airborne infection as a function of droplet diameter and pathogen type. Hence, the modeling results might be high-estimation without considering the evaporation and deposition processes.

There are a number of areas in which further research could strengthen the paper work. First, there is a need for sensitivity analysis using the Monte Carlo simulation technique associated with the more detailed data sets as inputs. Relationships between the input ranges and model output should then be assessed with stepwise regression in order to identify the relationship between output variability and input uncertainties and variabilities. On the basis of the results of the sensitivity analysis, research should be directed to those parameters that, if better characterized, could most effectively reduce variability in the results. Second, the deterministic model used in the present study was relatively easy to parameterize, yet it only captured the average behavior. In the future study, a stochastic model that allows an assessment of variability of the transmission behavior may be used to deal with the random nature of indoor aerosol transmission events.

In conclusion, this paper introduce a quantify framework for the viral kinetics of airborne influenza virus and exhaled pulmonary bioaerosol in that we adopted the mathematical modeling approaches for estimating the risk of infection. Viral kinetics expressed the competed results of human immunity ability with influenza virus generation. To involve the viral kinetics and different exposure parameters and environmental factors in a proposed school can be estimated the influenza infection risk. Eventually, a population dynamic model can illustrate the dynamics of infected person. Hence, each model is essential and plays the different role in disease transmission. However, this study cannot provide the relative importance with or without the viral kinetics than ventilation parameters or recovery rate. We only knew that viral kinetics in each experimental volunteer indeed affected the incubation rate and recovery rate in a specific individual scale.

From the aspect on inner infection mechanism to the process of exhaled pulmonary bioaerosol droplets, many questions must be resolved by future studies, including those related to the roles of other immune response properties of lung cells, like interferon (IFN) and CTLs immunity, the role of environmental conditions on expired bioaerosol number, and those control measures to diminish the number of expired bioaerosol particles. Thus, we have found that, viral kinetics and exhaled droplet size indeed affect indoor transmission dynamics of influenza virus based on our results. We believe that this framework can provide good estimation methods for overall aerosol transmission for influenza droplets while these questions are explored in the future studies.

Acknowledgements

This study was financially supported by National Science Council of Taiwan, Republic of China under Grant NSC 97-2313-B-002-017-MY3.

References

Anderson, R.M. and May, R.M. (1991) *Infectious Diseases of Humans: Dynamics and Control*, Oxford, Science Publications.

Atkinson, M.P. and Wein, L.M. (2008) Quantifying the routes of transmission for pandemic influenza, *Bull. Math. Biol.*, **70**, 820–867.

Baccam, P., Beauchemin, C., Macken, C.A., Hayden, F.G. and Perelson, A.S. (2006) Kinetics of influenza A virus infection in humans, *J. Virol.*, **80**, 7590–7599.

Beauchemin, C., Samuel, J. and Tuszynski, J. (2005) A simple cellular automaton model for influenza A viral infection, *J. Theor. Biol.*, **232**, 223–234.

Bocharov, G.A. and Romanyukha, A.A. (1994) Mathematical model of antiviral immune response, III: influenza A virus infection, *J. Theor. Biol.*, **167**, 323–360.

Chang, D.B. and Young, C.S. (2007) Simple scaling laws for influenza A rise time, duration, and severity, *J. Theor. Biol.*, **246**, 621–635.

Chen, S.C. and Liao, C.M. (2008) Modeling control measure efforts to reduce the impact of pandemic influenza among schoolchildren, *Epidemiol. Infect.*, **136**, 1035–1045.

Chen, S.C., Chang, C.F. and Liao, C.M. (2006) Predictive models of control strategies involved in containing indoor airborne infections, *Indoor Air*, **16**, 469–481.

Cole, E.C. and Cook, C.E. (1998) Characterization of infectious aerosols in health care facilities: An aid to effective engineering controls and preventive strategies, *Am. J. Infect. Control.*, **26**, 453–464.

Douglas, R.G. (1975) Influenza in man. In: Kilbourne, E.D. (ed.) *The Influenza*

Viruses and Influenza, New York, Academic Press, 375–447.
Duguid, J.P. (1945) The numbers and sites of origin of the droplets expelled during expiratory activities, *Edinb. Med. J.*, **52**, 385–401.
Duguid, J.P. (1946) The size and distribution of air-carriage of respiratory droplets and droplet-nuclei, *J. Hyg.*, **4**, 471–480.
Edwards, D.A., Man, J.C., Brand, P., Katstra, J.P., Sommerer, K., Stone, H.A., Nardell, E. and Scheuch, G. (2004) Inhaling to mitigate exhaled bioaerosols, *Proc. Natl Acad. Sci. USA*, **101**, 17383–17388.
Fennelly, K.P., Martyny, J.W., Fulton, K.E., Orme, I.M., Cave, D.M. and Heifets, L.B. (2004) Cough-generated aerosols of mycobacterium tuberculosis: a new method to study infectiousness, *Am. J. Respir. Crit. Care Med.*, **169**, 604–609.
Ferguson, N.M., Keeling, M.J., Edmunds, W.J., Gani, R., Grenfell, B.T., Anderson, R.M. and Leach, S. (2003) Planning for smallpox outbreaks, *Nature*, **425**, 681–685.
Fiegel, J., Clarke, R. and Edwards, D.A. (2004) Airborne infectious diseases and the suppression of pulmonary bioaerosols, *Drug Discov Today*, **11**, 51–57.
Gerrity, T.R., Lee, P.S., Hass, F.J., Marinelli, A., Werner, P. and Lourenco, R.V. (1979) Calculated deposition of inhaled particles in the airway generations of normal subjects, *J. Appl. Physiol.*, **47**, 867–873.
Hancioglu, B., Swigon, D. and Clermont, G. (2007) A dynamical model of human immune response to influenza A virus infection, *J. Theor. Biol.*, **246**, 70–86.
Handel, A., Longini, I.M. and Antia, R. (2007) Neuraminidase inhibitor resistance in influenza: assessing the danger of its generation and spread, *PLoS Computational Bio.*, **3**, 2456–2464.
Hayden, F.G., Fritz, R.S., Lobo, M.C., Alvord, W.G., Strober, W. and Straus, S.E. (1998) Local and systemic cytokine response during experimental human influenza A virus infection, *J. Clin. Invest.*, **101**, 643–649.
Hinds, W.C. (1999) *Aerosol Technology: Properties, Behavior, and Measurement of Airborne Particles*, New York, Wiley.
International Commission on Radiological Protection (1994) *Human Respiratory Tract Model for Radiological Protection*, a report of task group of the International Commission on Radiological Protection. ICRP Publication. Vol. 66. New York, Elsevier.
Knight, V. (1973) Airborne transmission and pulmonary deposition of respiratory viruses. In: Hers, J.F. and Winkles, K.C. (eds) *Airborne Transmission and Airborne Infections*. VIth International Symposium on Aerobiology, New York, Wiley, 175–182.
Li, Y., Leung, G.M., Tang, J.W., Yang, X., Chao, C.Y.H., Lin, J.Z., Lu, J.W., Nielsen, P.V., Niu, J., Qian, H., Sleigh, A.C., Su, H.J.J., Sundell, J., Wong, T.W. and Yuen, P.L. (2007) Role of ventilation in airborne transmission of infectious agents in the built environment – a multidisciplinary systematic review, *Indoor Air*, **17**, 2–18.
Liao, C.M., Chen, S.C. and Chang, C.F. (2008) Modeling respiratory infection control measure effects, *Epidemiol. Infect.*, **136**, 299–308.
Loudon, R.G. and Roberts, R.M. (1967) Relation between the airborne diameters of respiratory droplets and the diameter of the stains left after recovery, *Nature*, **213**, 95–96.
Marchuk, G.I., Petrov, R.V., Romanyukha, A.A. and Bocharov, G.A. (1991) Mathematical model of antiviral immune response. I. Data analysis, generalized picture construction and parameters evaluation for hepatitis B, *J. Theor. Biol.*, **151**, 1–40.
Murphy, B.R., Rennels, M.B. and Douglas, R.G. (1980) Evaluation of influenza A/Hong Kong/123/77(H1N1) *ts*-1A2 and cold-adapted recombinant viruses in seronegative adult volunteers, *Infect. Immun.*, **29**, 348–355.
Neumann, A.U., Lam, N.P., Dahari, H., Gretch, D.R., Wiley, T.E., Layden, T.J. and Perelson, A.S. (1998) Hepatitis C viral dynamics in vivo and the antiviral efficacy of interferon-alpha therapy, *Science*, **282**, 103–107.
Nicas, M., Nazaroff, W.W. and Hubbard, A. (2005) Toward understanding the risk of secondary airborne infection: emission of respiratory pathogens, *J. Occup. Environ. Hyg.*, **2**, 143–154.
Nowak, M.A. and Bangham, C.R.M. (1996) Population dynamics of immune responses to persistent viruses, *Science*, **272**, 74–79.
Nowak, M.A., Bonhoeffer, S., Hill, A.M., Boehme, R., Thomas, H.C. and McDade, H. (1996) Viral dynamics in hepatitis B virus infection, *Proc. Natl Acad. Sci. USA*, **93**, 4398–4402.
O'Grady, F. and Riley, R.L. (1963) Experimental airborne tuberculosis, *Adv. Tuberc. Res.*, **12**, 150–190.
Papineni, R.S. and Rosenthal, F.S. (1997) The size distribution of droplets in the exhaled breath of healthy human subjects, *J. Aerosol Med.*, **10**, 105–116.
Perelson, A.S. (2002) Modelling viral and immune system dynamics, *Nat. Rev. Immunol.*, **2**, 28–36.
Perelson, A.S., Kirschner, D.E. and Boer, R.J.D. (1993) Dynamics of HIV infection of $CD4^+$ T cells, *Math. Biosci.*, **114**, 81–125.
Perelson, A.S., Neumann, A.U., Markowitz, M., Leonard, J.M. and Ho, D.D. (1996) HIV-1 dynamics in vivo: virion clearance rate, infected cell life-span, and viral generation time, *Science*, **271**, 1582–1586.
Perelson, A.S., Essunger, P., Cao, Y., Vesanen, M., Hurley, A., Saksela, K., Markowitz, M. and Ho, D.D. (1997) Decay characteristics of HIV-1-infected compartments during combination therapy, *Nature*, **387**, 188–191.
Riley, E.C., Murphy, G. and Riley, R.L. (1978) Airborne spread of measles in a suburban elementary-school, *Am. J. Epidemiol.*, **107**, 421–432.
Rudnick, S.N. and Milton, D.K. (2003) Risk of indoor airborne infection transmission estimated from carbon dioxide concentration, *Indoor Air*, **13**, 421–432.
Snyder, M.H., Stephenson, E.H., Young, H., York, C.G., Tierney, E.L., London, W.T., Chanock, R.M. and Murphy, B.R. (1986) Infectivity and antigenicity of live avian-human influenza A reassortant virus: comparison of intranasal and aerosol routes in squirrel monkeys, *J. Infect. Dis.*, **154**, 709–711.
Stahlhofen, W., Rudolf, G. and James, A.C. (1989) Intercomparison of experimental regional aerosol deposition data, *J. Aerosol Med.*, **2**, 285–308.
Tang, J.W., Li, Y., Eames, I., Chan, P.K.S. and Ridgway, G.L. (2006) Factors involved in the aerosol transmission of infection and control of ventilation in healthcare premises, *J. Hosp. Infect.*, **64**, 100–114.
Wan, M.P., Chao, C.Y.H., Ng, Y.D., To, G.N.S. and Yu, W.C. (2007) Dispersion of expiratory droplets in a general hospital ward with ceiling mixing type mechanical ventilation system, *Aerosol Sci. Technol.*, **41**, 244–258.
Wells, W.F. (1934) On air-borne infection. Study II. Droplets and droplet nuclei, *Am. J. Hyg.*, **20**, 611–618.
Xie, X., Li, Y., Chwang, A.T.Y., Ho, P.L. and Seto, W.H. (2007) How far droplets can move in indoor environments-revisiting the Wells evaporation-falling curve, *Indoor Air*, **17**, 211–225.